

Mobile linkers on DNA-coated colloids: valency without patches

Stefano Angioletti-Uberti,^{1, a)} Patrick Varilly,² Bortolo M. Mognetti,³ and Daan Frenkel²

¹⁾*Department of Physics, Humboldt University of Berlin, Newtonstr.15, 12489 Berlin, Germany*

²⁾*Department of Chemistry, University of Cambridge, Lensfield Road, CB2 1EW Cambridge, UK*

³⁾*Center for Nonlinear Phenomena and Complex Systems, Université Libre de Bruxelles, Code Postal 231, Campus Plaine, B-1050 Brussels, Belgium*

Colloids coated with single-stranded DNA (ssDNA) can bind selectively to other colloids coated with complementary ssDNA. The fact that DNA-coated colloids (DNACCs) can bind to specific partners opens the prospect of making colloidal ‘molecules’. However, in order to design DNACC-based molecules, we must be able to control the valency of the colloids, i.e. the number of partners to which a given DNACC can bind. One obvious, but not very simple approach is to decorate the colloidal surface with patches of single-stranded DNA that selectively bind those on other colloids. Here we propose a design principle that exploits many-body effects to control the valency of otherwise isotropic colloids. Using a combination of theory and simulation, we show that we can tune the valency of colloids coated with mobile ssDNA, simply by tuning the non-specific repulsion between the particles. Our simulations show that the resulting effective interactions lead to low-valency colloids self-assembling in peculiar open structures, very different from those observed in DNACCs with immobile DNA linkers.

During the past two decades there has been substantial progress in the functionalization of colloidal particles with various ligand-receptor pairs such as complementary single-stranded DNA (ssDNA) sequences^{1,2}. ssDNA grafting makes it possible to control the specificity of inter-particle interactions³⁻⁵: two grafted ssDNA sequences bearing complementary Watson-Crick sequences can hybridise to form a double-stranded DNA (dsDNA) bridge between two particles, thus generating an effective attraction. In contrast, particles coated with non-complementary sequences do not attract. Exploiting this mechanism to tune colloidal interactions, DNA functionalisation has enabled the design of a variety of self-assembling nano-particle lattices⁶⁻⁸, thus opening the way towards new functional materials⁹.

However, at present our ability to design arbitrary structures is limited by the fact that it is not straightforward to control the coordination number (i.e. valency) in such colloidal structures. For instance, low-valency colloids can self-assemble into open structures¹⁰ that do not form if inter-particle interactions are pairwise additive and isotropic. On the atomic scale, carbon can form diamonds, where atoms are 4-coordinated, because carbon atoms have a well-defined electronic valency. In contrast, noble-gases interact through (nearly) pairwise additive interactions and only form dense structures, such as fcc and bcc.

If we wish colloidal particles to self-assemble into a diamond lattice, we need to control their valency. Colloidal diamond lattices are intensively studied because such crystals would facilitate production of photonics band gap materials^{11,12}. However, their direct self-assembly is currently hampered by the lack of simple ways to control colloidal valency.

Considerable progress has been made in the (multi-step) synthesis of colloids with a well-defined valency encoded through the careful positioning of ssDNA linkers in patches at specific positions. Wang *et al*¹³ have shown that it is possible to produce colloids with patches in precise locations; DNA can be grafted selectively onto these patches. In this Letter, we present calculations that indicate that it should be possible to enforce the valency of colloidal particles without “statically” encoding it in their structure. Instead, many-body effects naturally arising in DNACCs with mobile linkers can be exploited to this purpose. Moreover we show that valency control can be tuned by changing the grafting density of inert strands, temperature or salt concentration.

As an illustration we consider a binary system of colloids, A and B (see Fig. 1), covered with mobile n_α and n_β DNA strands. Each strand terminates in a short sequence of complementary ssDNA, α and β . Such colloids have been previously synthesised in various ways, as described in Refs.^{14,15}. When the suspension is cooled below a specific (sequence-dependent) temperature, the ssDNA will hybridise with its complement, forming bonds between the DNACCs. Reliable techniques exist^{16,17} to predict the strength of attraction between A and B colloids as a function of temperature. Same-type colloids (i.e. $A - A$ or $B - B$ pairs) repel each other due to the steric repulsion between non-binding ssDNA.

The interactions between colloids coated with mobile ssDNA are not pairwise additive. Consider two DNACCs, A and B_1 , brought to a distance where hybridisation is possible. These two colloids will experience an attraction with a

^{a)}Electronic mail: sangiole@physik.hu-berlin.de; Corresponding author

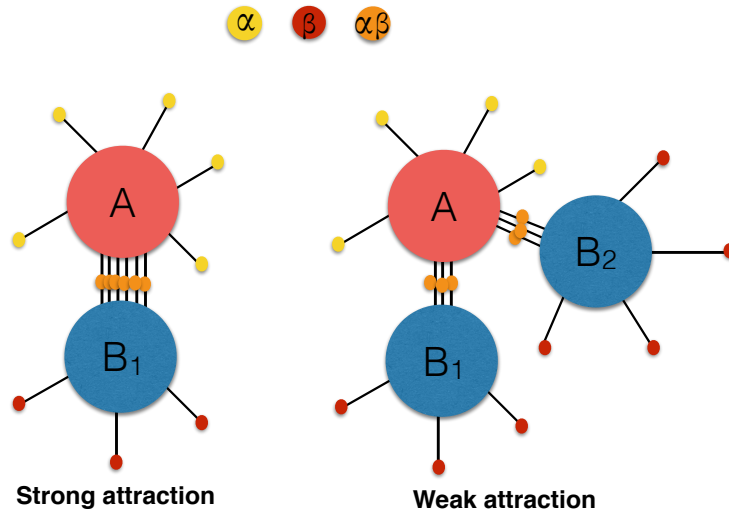


FIG. 1: Schematic representation of our system. Colloid A bears DNA sequences that are complementary to those on B. Given that a fixed number of linking DNA exists, when multiple possible partners are present the total number of bonds between colloids decreases, hence their binding free-energy. This is the basis of the multi-body effect controlling valency.

strength that increases with the number of bonds. If a second colloid of type B (here, B_2) is inserted in the system at the same distance from colloid A as colloid B_1 (Fig. 1), any of the mobile DNA strands on A can now hybridise with either B_1 or B_2 . The symmetry of the problem requires that on average the same number of bonds will form between A and B_1 and A and B_2 . Since the strength of the effective inter-particle interaction is an increasing function of the number of bonds and given that there is a finite number of strands to form bonds, the presence of a third colloid lowers the effective attraction between two particles. This many-body effect is at the basis of the mechanism controlling valency in this class of colloids. However, and this is our key point, the decrease of the binding strength per bond with the number of neighbours is *not* enough to control the colloidal valency, as the maximum number of neighbours is determined by the total cluster interaction energy: each new bonding partner makes inter-particle interactions weaker but adds one more interacting pair. In the absence of non-specific repulsions, the highest coordination numbers are most favourable. However, if we add non-specific repulsions to the colloidal interactions, we can tune the optimal coordination number.

To make our argument quantitative, we calculate the effective interactions in different clusters. To this end, we need an expression for the interaction free-energy of a cluster where the colloids positions are fixed at arbitrary positions. We then relax the fixed-positions constraint and perform Monte Carlo (MC) simulations where the colloids positions are allowed to achieve their equilibrium distribution.

Our expression for the effective interaction between DNACCs is based on the mean-field approach developed in Refs.^{16,17}, and used to describe a variety of systems^{18–21}. As shown in ref.¹⁷, this approach yields quantitative agreement with MC simulations.

Ref.¹⁷ showed that the attractive part of the effective interaction free-energy induced by a system of ligand-receptor pairs (e.g. complementary DNA-strands) with bonding energies $\beta\Delta G_{ij}$ (where i and j label two specific binding

partners) is approximated remarkably well by the following expression:

$$\beta F_{\text{att}} = \sum_i \ln p_i + \sum_{i < j} p_{ij} \quad (1)$$

where p_i is the probability that linker i is unbound and p_{ij} is the probability that linkers i and j form a bond. These quantities are given by solving the following set of equations:

$$p_{ij} = p_i p_j e^{-\beta \Delta G_{ij}}, \quad (2)$$

$$p_i = 1 - \sum_j p_{ij} \quad (3)$$

where $\Delta G_{ij}(\mathbf{r}_i, \mathbf{r}_j)$ is the free energy for the formation of a single bond between the $i - j$ pair. The latter can be rewritten in a more insightful form as^{16,22}:

$$\beta \Delta G_{ij}(\mathbf{r}_i, \mathbf{r}_j) = \beta \Delta G_0 + \beta \Delta G_{\text{conf}}(\mathbf{r}_i, \mathbf{r}_j) \quad (4)$$

where $\beta \Delta G_0$ is the hybridisation free-energy for two DNA strands in solution. $\beta \Delta G_0$ depends only on DNA sequence and is a function of temperature and salt concentration^{23,24}. $\beta \Delta G_{\text{conf}}(\mathbf{r}_i, \mathbf{r}_j)$, an explicit function of the grafting points $\mathbf{r}_i, \mathbf{r}_j$, is the configurational cost associated with the bond formation, and has been previously quantified both for single and double-stranded DNA^{16,23}.

For the case of mobile DNA, all strands with the same recognition sequence that reside on the same colloid are equivalent since they cannot be distinguished by their grafting position. In this case, the correct procedure is to replace $e^{-\beta \Delta G_{ij}(\mathbf{r}_i, \mathbf{r}_j)}$ by its average over all possible grafting points. Hence, the effective, single-bond strength between types α and β residing on colloids A and B , respectively, will be given by

$$\begin{aligned} \Xi_{\alpha\beta}(\mathbf{R}_A, \mathbf{R}_B) &= \langle \exp(-\beta \Delta G_{\alpha\beta}) \rangle_{|\mathbf{R}_A, \mathbf{R}_B} \\ &= \frac{\int_{S_A, S_B} \exp[-\beta \Delta G_{\alpha\beta}] d\mathbf{r}_\alpha d\mathbf{r}_\beta}{S_A S_B} \end{aligned} \quad (5)$$

where the average is taken keeping the centre of colloid $A(B)$ at $\mathbf{R}_{A(B)}$ fixed and $S_{A(B)}$ is the area of the colloid. In Eq. 5 we use greek subscripts to label a strand type (rather than *specific* strands as in Eqs. 3,2). We follow this convention from now on. Using Eqs. 2, 3 to replace p_{ij} in Eq. 1, and considering that strands of the same type are equivalent and hence have the same value for Ξ , we obtain:

$$\begin{cases} p_\alpha + \sum_{\gamma=1}^{N_{\text{types}}} n_\gamma p_\alpha p_\gamma \Xi_{\alpha\gamma}(\mathbf{R}_\alpha, \mathbf{R}_\gamma) = 1 \\ \dots \\ p_{N_{\text{types}}} + \sum_{\gamma=1}^{N_{\text{types}}} n_\gamma p_{N_{\text{types}}} p_\gamma \Xi_{N_{\text{types}}\gamma}(\mathbf{R}_{N_{\text{types}}}, \mathbf{R}_\gamma) = 1. \end{cases} \quad (6)$$

and

$$\beta F = \sum_\gamma n_\gamma [\ln p_\gamma + 1/2 (1 - p_\gamma)]. \quad (7)$$

Eq. 6 is a system of N_{types} equations, one for each possible non-equivalent strand in the system: its solution is an explicit function of all colloidal positions $\{\mathbf{R}\}$. Hence, if two strands cannot bind because they are grafted on distant colloids, $\Xi = 0$ and the sum over γ in Eq. 6 effectively runs only on strand types on neighbouring colloids.

Eqns. 6, 7 are key results of this paper. They allow to calculate the bond-mediated binding energy for any two generic objects interacting via mobile linkers. We show in the SI that for mobile linkers these formulas become exact in the limit of large numbers of linkers.

Let us first consider clusters made of 1 colloid of type A surrounded by N_B colloids of type B at equivalent positions (by symmetry only two types of strands are present, α and β) for which Eqs. 6,7 become:

$$\begin{cases} p_\alpha + N_B n_\beta p_\alpha p_\beta \Xi = 1 \\ p_\beta + n_\alpha p_\alpha p_\beta \Xi = 1 \end{cases} \quad (8)$$

and

$$\beta F_{clus}^{bond} = n_\alpha (\ln p_\alpha + 1/2 - p_\alpha/2) + N_B n_\beta (\ln p_\beta + 1/2 - p_\beta/2). \quad (9)$$

Eq. 9 (closed-form solution in SI) gives only the contribution due to bonds formation between ligands, and is purely attractive. For typical DNACCs realisations, other terms due to van-der-Waals forces or electrostatic interactions are negligible at the binding distance between colloids of a few nanometers imposed by the DNA length²². Hence, their effect can be safely disregarded. However, other terms due for example to the presence of inert DNA-strands or other polymers can still be relevant. These polymers act as steric stabilisers via excluded volume interactions, giving a repulsive energy of general form:

$$\beta F_{rep} = -k_B T \ln \left(\frac{\Omega(\{\mathbf{r}_i\})}{\Omega_{free}} \right) \quad (10)$$

where $\Omega(\{\mathbf{r}_i\})$ is the partition function counting all accessible states of the polymers given the positions of the colloids $\{\mathbf{R}\}$ and Ω_{free} is the same partition function when the colloids are at infinite separation. As for $\beta \Delta G_{cnf}$, the contribution due to Eq. 11 can be calculated exactly for selected polymeric architectures or otherwise computed with MC simulations¹⁶.

To illustrate the effect of non-specific repulsion, first consider the case that F_{rep} between two colloids has a constant value F_{rep}^{min} . The total energy of a $1A + N_B B$ cluster then has an additional term $N_B F_{rep}^{min}$. Added to Eq. 9, we obtain a closed analytical expression for the free-energy of a cluster $F_{clus}(n_\alpha, n_\beta, N_B, \Xi, F_{rep}^{min})$. If we divide F_{clus} by the number of neighbours, we obtain the total energy per bonding pair $F_{pair} = F_{clus}/N_B$ (Eq. 18-22 in the SI).

Fig. 2 confirms that F_{pair} is *always* an increasing function of the number of colloids, hence attraction in an $A-B$ pair becomes weaker by increasing the number of neighbours. However, it is F_{clus} that controls the valency distribution function. Without a local minimum in F_{clus} , the latter peaks at the highest possible coordination number (i.e. 12 for equal-sized spheres). A minimum in F_{clus} appears only if a finite repulsion βF_{rep}^{min} is present, in which case the valency distribution peaks at a lower value dependent on βF_{rep}^{min} (dashed and continuous curves in the inset), suggesting a viable route to tune DNACCs' valency.

In practice, the repulsive energy at the equilibrium distance can be controlled by coating colloids with inert DNA strands or other polymers that are somewhat longer than the 'sticky' DNA strands¹⁹. Based on these results, we expect that in a realistic system of DNACCs with mobile linkers one can control the average valency by varying temperature or salt concentration. We also expect, based on Eqs. 5,11, that the specific value of ΔG_0 at which a particular valency is stabilised will depend on the grafting density and the size of the colloids, since both these parameters enter in our equations.

To demonstrate this, we performed MC simulations of an equimolar $A : B$ mixture of colloids that can move freely. βF_{rep} was calculated by using Eq. 11 and considering the case of mobile strands (details of its calculation are reported in the SI). We stress that our outcomes are insensitive to the precise choice of F_{rep} . We take two specific realisation of the system, differing in the presence or absence of long inert strands. Each colloid is modelled as a hard sphere with a radius $R = 100$ nm on which 70 rigid, double stranded DNA of length $L = 20$ nm terminating with a short single-stranded DNA sequence are grafted (as in the plots for Fig. 2). In the system with inert strands, 40 additional strands of dsDNA of length 60 nm are added. Since $L \ll \xi_p$, the persistence length of ds-DNA, linkers can be described as rigid rods²², for which both the contribution to the repulsive energy as well DG^{cnf} for mobile linkers can be calculated analytically given the colloids' positions (see the SI). This model for the DNA-construct corresponds to the experimental realisation described in^{22,25-27}. In each run, 10^5 MC sweeps *per* particles are made, starting with 100 colloids in random positions at packing fraction 0.05 and at various values of ΔG_0 . Each trial move consists of a random displacement $\mathbf{r} \in [-0.25L, 0.25L]^3$, and the total free-energy recalculated using Eqs. 6,7 under periodic boundary conditions. The analysis was performed every 100 sweeps *per* particle, and the valency distribution function (φ in the inset of Fig. 2) was calculated using the maximum bonding distance, i.e. $2L$ for rigid rods.

Results are presented in Fig. 3, for the case with (left) and without (right) inert strands, corresponding to $F_{rep}^{min} > 0$ and $F_{rep}^{min} = 0$, respectively.

These results support the conclusions based on the simpler analytical model derived for the quenched-cluster system: repulsion plays an important role in stabilising low-valency structures. In particular, higher repulsion shifts the average valency to lower values. As predicted by our simplified model, the valency probability distribution can be tuned by

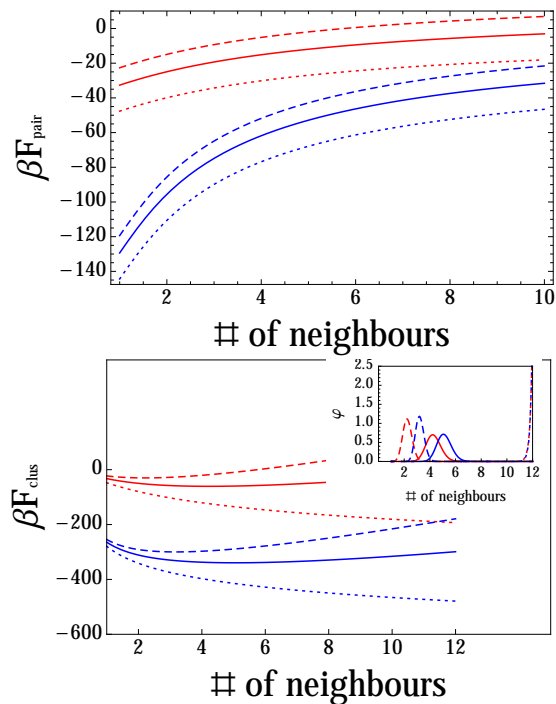


FIG. 2: Energy per pair (βF_{pair} , above) and cluster energy (βF_{clus} , below) for a cluster in our system of DNACCs with mobile strands. Same color (online version) means same value of ΔG_0 . Lines of different style represent different values of βF_{rep}^{min} (0, 15 and 25 for dotted, continuous and dashed lines, respectively). Lines of different colours have been shifted by an irrelevant constant to facilitate comparison. The inset shows the valency probability distributions φ , which peak at low valency if $F_{rep}^{min} > 0$.

changing ΔG_0 , i.e. temperature or salt concentration. The observed valency distribution for colloids without inert strands is relatively broad, which can mainly be attributed to finite size effects in our system. Although we did not calculate the equilibrium phase diagram for this system, all observed structures assemble quickly and spontaneously from a random configuration and remain stable, suggesting at least metastability. Without inert strands a compact and well ordered crystal forms, whereas the open structures observed in their presence lack long-range order. This is not necessarily required to achieve interesting functional properties: low valency was shown to be enough to obtain structures with a proper, 3-dimensional photonic band-gap²⁸.

Finally, we note that Feng *et al*¹⁵ have reported the experimental observation of low-valency structures of deformable, micron-sized oil droplets coated with mobile DNA. In this system, the repulsion mechanism is droplet deformation. As we have not applied our theory to this case, we cannot yet conclude whether droplet deformation alone can limit valency.

To conclude, in this paper we have studied the collective behaviour of a suspensions of binary *isotropic* colloids functionalised by mobile linkers. We showed how the interaction parameters can be tuned to induce the self-assembly of aggregates exhibiting a desired number of neighbours. Our model indicates that such a valency control can be achieved by changing the non-specific repulsion between colloids and is a function of temperature and salt concentration. We also derive an explicit formula for the bonding-energy of a system of mobile linkers, provide the set of self-consistent equations needed to calculate it, and show how they can be used to drive an MC algorithm to efficiently sample the DNA-mediated free-energy. Hence beyond motivating experimental work towards the design of low valency structures, we provide tools to model other systems interacting via reversible mobile binders: an obvious example is the interaction between lipid vesicles²⁹, or functionalised particles with cell membranes, whose interaction strongly depends on ligand-receptor bonds formation³⁰.

I. ACKNOWLEDGMENTS

S.A-U acknowledges support from the Alexander von Humboldt Foundation via a Postdoctoral Fellowship. This work was supported by the European Research Council Advanced Grant 227758, the Wolfson Merit Award 2007/R3

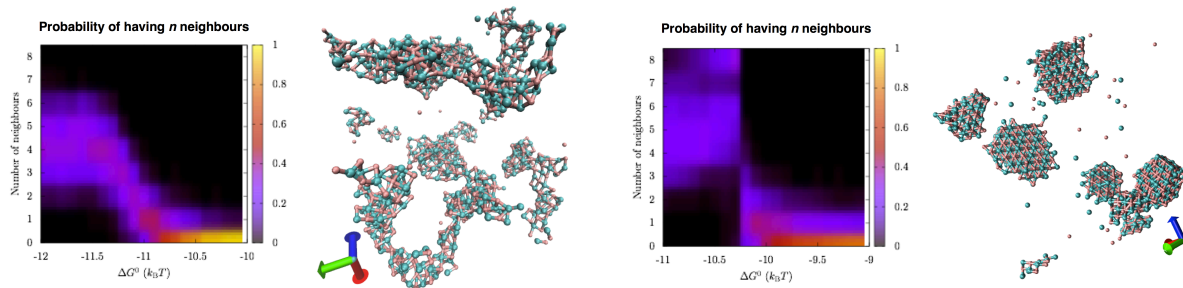


FIG. 3: Valency distribution as a function of $\beta\Delta G_0$ for colloids with (left) and without (right) inert strands. The repulsive free-energy at the equilibrium distance between colloids has an appreciable value only when inert strands are present, and is basically zero otherwise. The snapshots show typical configurations found at low $\beta\Delta G_0$ in the two cases, where the system either assembles open structures of tetrahedral coordination (left, with inert strands) or a more compact NaCl structure (right, no inert strands).

of the Royal Society of London and the Engineering and Physical Sciences Research Council Programme Grant EP/I001352/1. P.V. has been supported by a Marie Curie International Incoming Fellowship of the European Community's Seventh Framework Programme under contract number PIFI-GA-2011-300045, and by a Tizard Junior Research Fellowship from Churchill College.

- ¹C. A. Mirkin, R. C. Letsinger, R. C. Mucic, and J. J. Storhoff, *Nature* **382**, 607 (1996).
- ²A. P. Alivisatos, K. P. Johnsson, X. Peng, T. E. Wilson, C. J. Loweth, M. P. Bruchez, and P. G. Schultz, *Nature* **382**, 609 (1996).
- ³D. Nykypanchuk, M. M. Maye, D. van der Lelie, and O. Gang, *Langmuir* **23**, 6305 (2007), <http://pubs.acs.org/doi/pdf/10.1021/la0637566>.
- ⁴P. L. Biancaniello, A. J. Kim, and J. C. Crocker, *Phys. Rev. Lett.* **94**, 058302 (2005).
- ⁵A. J. Kim, P. L. Biancaniello, and J. C. Crocker, *Langmuir* **22**, 1991 (2006), <http://pubs.acs.org/doi/pdf/10.1021/la0528955>.
- ⁶S. Y. Park, A. K. R. Lytton-Jean, B. Lee, S. Weigand, G. C. Schatz, and C. A. Mirkin, *Nature Materials* **451**, 553 (2008).
- ⁷D. Nykypanchuk, M. M. Maye, D. van der Lelie, and O. Gang, *Nature Materials* **451**, 549 (2008).
- ⁸R. Macfarlane, B. Lee, M. Jones, N. Harris, G. Schatz, and C. A. Mirkin, *Science* **334**, 204 (2011).
- ⁹Y. Zhang, L. Fang, K. Yager, D. van der Lelie, and O. Gang, *Nature Nanotechnology* **8**, 865 (2013).
- ¹⁰F. Romano, E. Sanz, and F. Sciortino, *The Journal of Chemical Physics* **134**, 174502 (2011).
- ¹¹J. D. Joannopoulos, P. R. Villeneuve, and S. Fan, *Nature* **386**, 143 (1997).
- ¹²S. Linden, C. Enkrich, M. Wegener, J. Zhou, T. Koschny, and C. M. Soukoulis, *Science* **306**, 1351 (2004), <http://www.sciencemag.org/content/306/5700/1351.full.pdf>.
- ¹³Y. Wang, Y. Wang, D. R., V. N. Manoharan, L. Feng, A. D. Hollingsworth, M. Weck, and D. J. Pine, *Nature* **491**, 51 (2012).
- ¹⁴S. A. J. van der Meulen and M. E. Leunissen, *Journal of the American Chemical Society* **135**, 15129 (2013), <http://pubs.acs.org/doi/pdf/10.1021/ja406226b>.
- ¹⁵L. Feng, L.-L. Pontani, R. Dreyfus, P. Chaikin, and J. Brujic, *Soft Matter* **9**, 9816 (2013).
- ¹⁶P. Varilly, S. Angioletti-Uberti, B. M. Mognetti, and D. Frenkel, *The Journal of Chemical Physics* **137**, 094108 (2012).
- ¹⁷S. Angioletti-Uberti, P. Varilly, B. M. Mognetti, A. Tkachenko, and D. Frenkel, *The Journal of Chemical Physics* **138**, 021102 (2013).

- ¹⁸B. M. Mognetti, P. Varilly, S. Angioletti-Uberti, F. Martinez-Veracoechea, J. Dobnikar, M. Leunissen, and D. Frenkel, Proceedings of the National Academy of Sciences **109** (2012), doi/10.1073/pnas.1119991109.
- ¹⁹S. Angioletti-Uberti, B. M. Mognetti, and D. Frenkel, Nature Materials **11**, 518 (2012).
- ²⁰F. Martinez Veracoechea, B. M. Mognetti, S. Angioletti-Uberti, P. Varilly, D. Frenkel, and J. Dobnikar, Soft Matter **10**, 3463 (2014).
- ²¹B. M. Mognetti, M. E. Leunissen, and D. Frenkel, Soft Matter **8**, 2213 (2012).
- ²²M. E. Leunissen and D. Frenkel, Journal of Chemical Physics **134**, 084702 (2011).
- ²³L. Di Michele, B. M. Mognetti, T. Yanagishima, P. Varilly, Z. Ruff, D. Frenkel, and E. Eiser, Journal of the American Chemical Society **136**, 6538 (2014), <http://pubs.acs.org/doi/pdf/10.1021/ja500027v>.
- ²⁴J. SantaLucia, Proceedings of the National Academy of Sciences of the United States of America **95**, 1460 (1998), <http://www.pnas.org/content/95/4/1460.full.pdf+html>.
- ²⁵M. E. Leunissen, R. Dreyfus, F. C. Cheong, D. G. Grier, R. Sha, N. C. Seeman, and P. M. Chaikin, Nature Materials **8**, 590 (2009).
- ²⁶M. E. Leunissen, R. Dreyfus, R. Sha, N. C. Seeman, and P. M. Chaikin, Journal of the American Chemical Society **132**, 1903 (2010), PMID: 20095643, <http://pubs.acs.org/doi/pdf/10.1021/ja907919j>.
- ²⁷R. Dreyfus, M. E. Leunissen, R. Sha, A. V. Tkachenko, N. C. Seeman, D. J. Pine, and P. M. Chaikin, Phys. Rev. Lett. **102**, 048301 (2009).
- ²⁸K. Edagawa, S. Kanoko, and M. Notomi, Phys. Rev. Lett. **100**, 013901 (2008).
- ²⁹D. Serien, C. Grimm, J. Liescher, A. Herrmann, and A. Arbuzova, New J. Chem. , (2014).
- ³⁰G. Bell, Science **200** (1978).

II. SUPPLEMENTARY INFORMATION

A. Accurate approximation for calculating the repulsive free-energy

When colloids are functionalised with grafted polymers under good solvent conditions, polymeric chains act as steric stabilisers via excluded volume interactions. More precisely, they induce a repulsive free-energy between colloids due to the fact that the impenetrable colloids limit the amount of configurations the chains can attain, hence reducing the free-energy of the system. Formally, this can be written as:

$$\beta F_{rep} = -k_B T \ln \left(\frac{\Omega(\{\mathbf{R}_I\})}{\Omega_{tot}} \right) \quad (11)$$

where $\Omega(\{\mathbf{R}_I\})$ is the partition function counting all accessible states of the polymers given the positions of all other colloids in the system $\{\mathbf{R}_I\}$ (see note⁷) and Ω_{tot} is $\Omega(\{\mathbf{R}_I\})$ for isolated colloids (see Fig. 4a for reference). We take the polymers to be ideal, and hence $\Omega(\{\mathbf{R}_I\})$ simply counts the number of available geometric states, which are all considered to have exactly the same energy and hence the same weight, i.e. the system is athermal. In our model, the polymer is a stiff, double-stranded (ds) DNA of length ℓ_i terminating with a small, point-like recognition sequence. Since we assume $\ell_i \ll \xi_i$ (ξ_i being the persistence length of dsDNA), we can describe it as a rigid rod whose grafting point can move on the surface. As we are about to show, in this case a very accurate analytic approximation exists for Eq. 11, which becomes better and better in the limit $\ell/R \rightarrow 0$, R being the radius of the colloid on which the strand is grafted.

Let us first introduce a quantity, $P(\mathbf{r})$, defined as the probability that the end point of our rod (i.e that not grafted to the surface) is at a position \mathbf{r} (see Fig. 4b for reference). $P(\mathbf{r})$ is given by the following expression:

$$P(\mathbf{r}) = \int_{-\pi}^{\pi} \frac{2\pi R^2 \sin(\theta) d\theta}{4\pi R^2} \frac{\delta(|\mathbf{r} - \mathbf{r}'| - \ell)}{2\pi\ell^2} \Theta[(\mathbf{r} - \mathbf{r}') \cdot (\mathbf{r}' - \mathbf{O})] \quad (12)$$

where the Dirac delta function takes care of fixing the rod length and the Heaviside step function makes sure that the rod does not penetrate the colloid on which is coated. The integral in Eq. 12 can be calculated giving the following result:

$$P(\mathbf{r}) = \begin{cases} \frac{1}{4\pi R\ell r} & R^2 + \ell^2 < r^2 < (R + \ell)^2; \\ 0 & \text{otherwise.} \end{cases} \quad (13)$$

which, for small $\ell/R \rightarrow 0$, can be further approximated as

$$P(\mathbf{r}) = \begin{cases} \frac{1}{4\pi R^2 \ell} & R^2 + \ell^2 < r^2 < (R + \ell)^2; \\ 0 & \text{otherwise.} \end{cases} \quad (14)$$

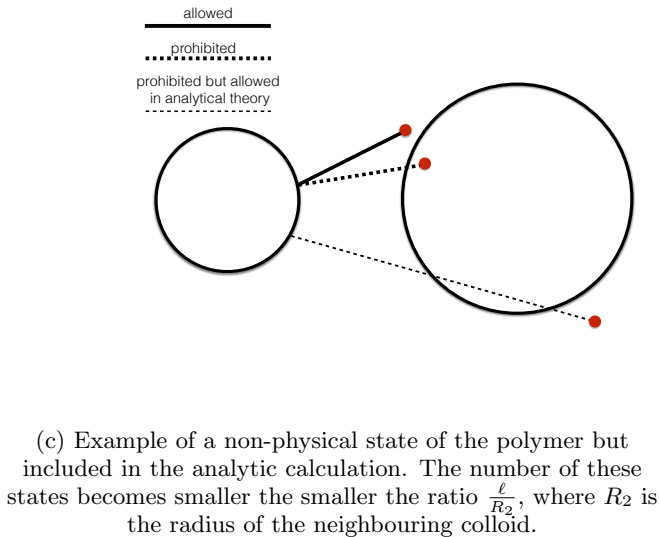
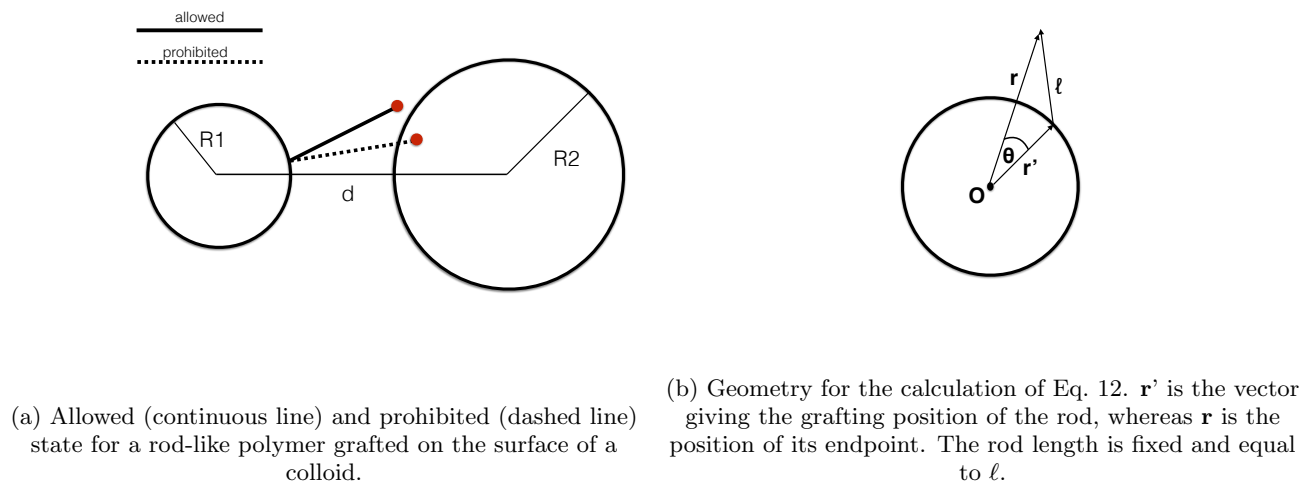


FIG. 4

i.e. $P(\mathbf{r})$ is *uniform*. Our first approximation will be to take this uniform value for $P(\mathbf{r})$. Let us now make a second approximation, whose validity also increases in the limit $\ell/R_2 \rightarrow 0$ (where R_2 now labels a colloid among the neighbours on which the polymer is grafted). We will count as allowed states for our rod all those for which its end-point is not inside a neighbouring colloid (see Fig. 4 for reference). Note that within this approximation we are (wrongly) counting as allowed configurations those where the rod overlaps a neighbour for a fraction which does not include the end point (see 4c). Given that we take a flat probability distribution, the number of these states is simply proportional to the overlap volume $V_{overlap}$ between a sphere of radius $R_1 = R + \ell$ and that of a sphere of radius R_2 , given by:

$$V_{overlap}(R_1, R_2, d) = \frac{\pi}{12d}(R_1 + R_2 - d)^2 (d^2 + 2d(R_1 + R_2) - 3(R_1^2 + R_2^2) + 6R_1R_2). \quad (15)$$

Since the total number of states available for a grafted rod when no other colloids are present is proportional to the volume accessible to its end-point $V_{tot} = 4\pi R^2 \ell$, the following equation holds:

$$\frac{\Omega(\{\mathbf{r}_i\})}{\Omega_{tot}} \approx V_{free}/V_{tot} = \frac{V_{tot} - \sum_{neighbours} V_{overlap}}{V_{tot}} \quad (16)$$

hence, considering that rods behave as ideal (i.e. they do not interact with each other), we find the following final expression for the repulsive free-energy induced by n_j mobile rods grafted on a surface of a colloid due to the presence of its neighbours with positions \mathbf{R}_i :

$$\begin{aligned} \beta F_{rep} &= -k_B T \ln \left(\prod_{j=1}^{n_j} \frac{\Omega(\ell_j, \{\mathbf{R}_i\})}{\Omega_{tot}} \right) \\ &= -k_B T \sum_j \ln \left(1 - \frac{\sum_{i=1}^{N_{colloid}} V_{overlap}(R + \ell_j, R_i, d)}{4\pi R^2 \ell} \right). \end{aligned} \quad (17)$$

To appreciate the difference between the analytic approximation and a numerically accurate Monte Carlo estimation of F_{rep} , we report in Fig. 5 the repulsive free-energy between two colloids calculated in both ways for two colloids coated with 70 strands of either length $\ell = 0.2 R_C$ or $\ell = 0.6 R_C$, as in our simulations.

Whereas the difference is negligible for the short rods, it starts to become relevant for the longer ones. However, we observe that a simple rescaling procedure can be used to get accurate results, i.e. one can take $F_{rep}^{scaled} = F_{rep}^{analytic}/\alpha$ and the data reproduces the accurate numerical results for all colloids distances d (for the longer strands $\alpha \approx 1.5$, note that its value depends on the specific ℓ/R ratio). This is equivalent to saying that, by using the analytical estimate for F_{rep} , we are effectively simulating a system whose grafting density is about 1.5 times larger than the real one. For the sake of computational efficiency and reproducibility, in our simulations we always use the analytic approximation. Hence, if one intends to experimentally replicate the system, a higher coverage should be used (for the value of α in our model, this is still well in the range of values used in experiments).

As for F_{rep} , a similar approach can be taken in our system to calculate $\beta\Delta G^{cnf}$ (Eq. 4 in the main text), i.e. the entropic configurational penalty to form a bond between two DNA strands. In our case, $\beta\Delta G^{cnf}$ is the configurational free-energy penalty to confine the end of two grafted rods at the same location (or, better, within a bonding volume $v_0^{16,21}$). This is given by¹⁶:

$$\beta\Delta G^{cnf} = -\log \left(\frac{1}{\rho_0} \frac{\Omega_{ij}}{\Omega_i \Omega_j} \right) \quad (18)$$

where ρ_0 is the standard concentration, 1 M, Ω_{ij} is the phase space allowed for two strands i and j grafted at colloid I and J respectively and bound to each other, and $\Omega_{i(j)}$ the phase space allowed for two grafted but unbound strands, i.e. V_{free} calculated previously. Using exactly arguments and approximations previously used to calculate F_{rep} , the following holds:

$$\begin{aligned} \Omega_{ij} &= V_{overlap}(R_I + L_i, R_J + L_j, d) - V_{overlap}(R_I + L_i, R_J, d) \\ &\quad - V_{overlap}(R_I, R_J + L_j, d) \end{aligned} \quad (19)$$

B. Large number of linkers limit of the bonding free-energy in the presence of mobile linkers:

In this section we show that the set of self-consistent equations developed for DNA coated colloids (Eqs. 6 in the manuscript), and the free energy used (Eq. 7 in the manuscript) are exact when the number of DNA-strands (linkers, from now on) becomes large. This is shown by using a saddle-point approximation.

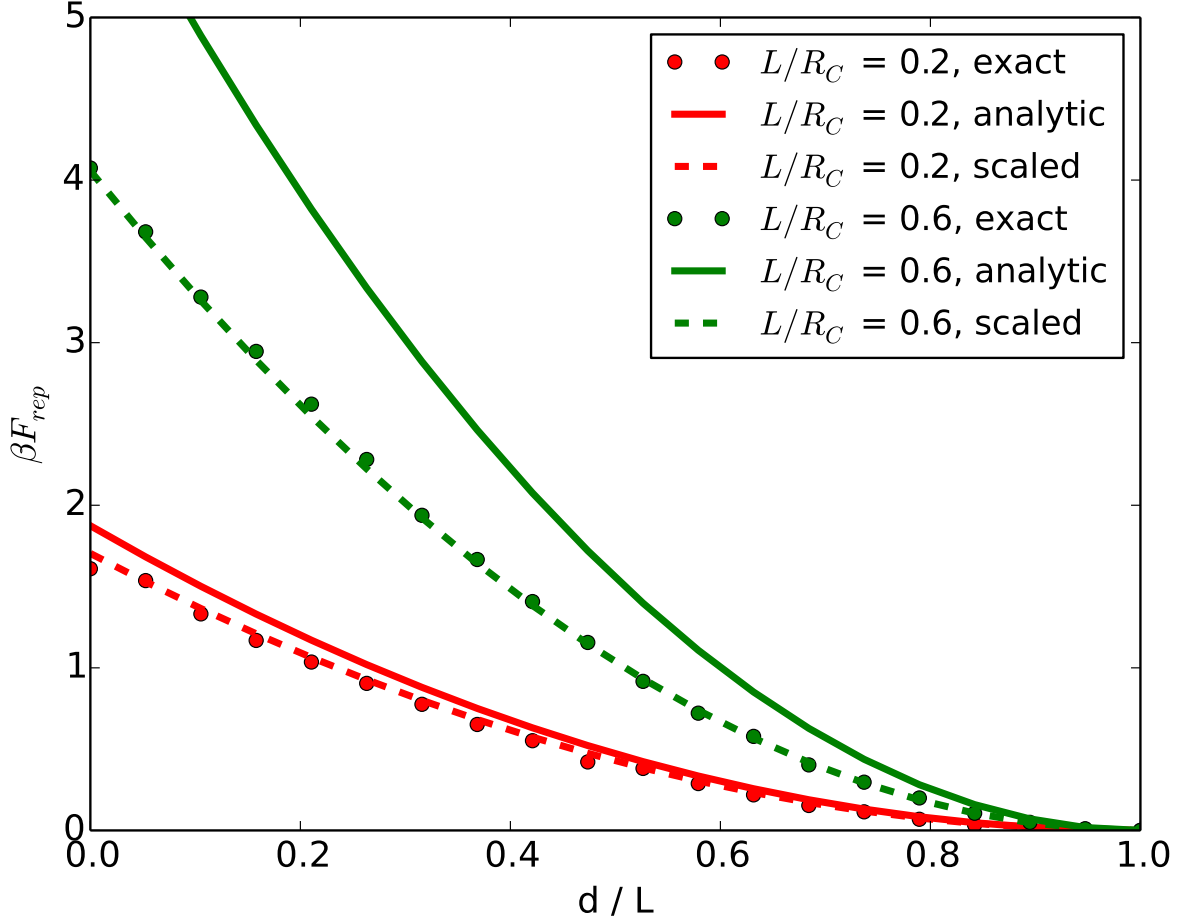


FIG. 5: Comparison of the numerically accurate Monte Carlo evaluation of F_{rep} as given by Eq. 11 (circles) and the analytic approximation given by Eq. 17, with and without scaling to adjust it (dashed and full lines, respectively). Green is for long strands ($L/R_C = 0.6$) whereas red is for the shorter ones ($L/R_C = 0.2$). As expected, whereas the analytic approximation very well reproduces the Monte Carlo data for the shorter strands, a considerable difference appear for the longer ones. However, a simple rescaling procedure is sufficient to reproduce the numerical estimation with high accuracy.

The DNA partition function for a set of colloids at fixed positions is given by

$$Z = \sum_{\{x_{\alpha\beta}\}} W(\{x_{\alpha\beta}\}) (\Xi_{\alpha\beta})^{\sum x_{\alpha\beta}},$$

$$W(\{x_{\alpha\beta}\}) = \prod_{\alpha} \frac{n_{\alpha}!}{(n_{\alpha} - \sum_{\beta} x_{\alpha\beta})!} \prod_{\alpha < \beta} \frac{1}{x_{\alpha\beta}!}, \quad (20)$$

where the Ξ factors have been defined in Manuscript Eq. 5 (here we omit the dependence of Ξ on the colloids' position). $W(\{x_{\alpha\beta}\})$ counts all the possible combinations of DNA–DNA hybridisation resulting in $x_{\alpha\beta}$ bridges between particle α and particle β with $1 \leq \alpha, \beta \leq N_{\text{type}}$ (Fig. 6a). In the definition of W (Eq. 20) the first product is taken on all the type of linkers while the second on all possible pairs of types. Linkers are of different types if they are either grafted on different colloids or have a different recognition sequences. The partition function Z is then defined as in Eq. 20 taking the sum on all the possible sets of pairs consistent with a total number of strands in the system weighted with the total hybridisation free energy (as given by Manuscript Eq. 5).

The derivation of $W(\{x_{\alpha\beta}\})$ is shown in Fig. 6(b–d) for the case in which different types correspond to different

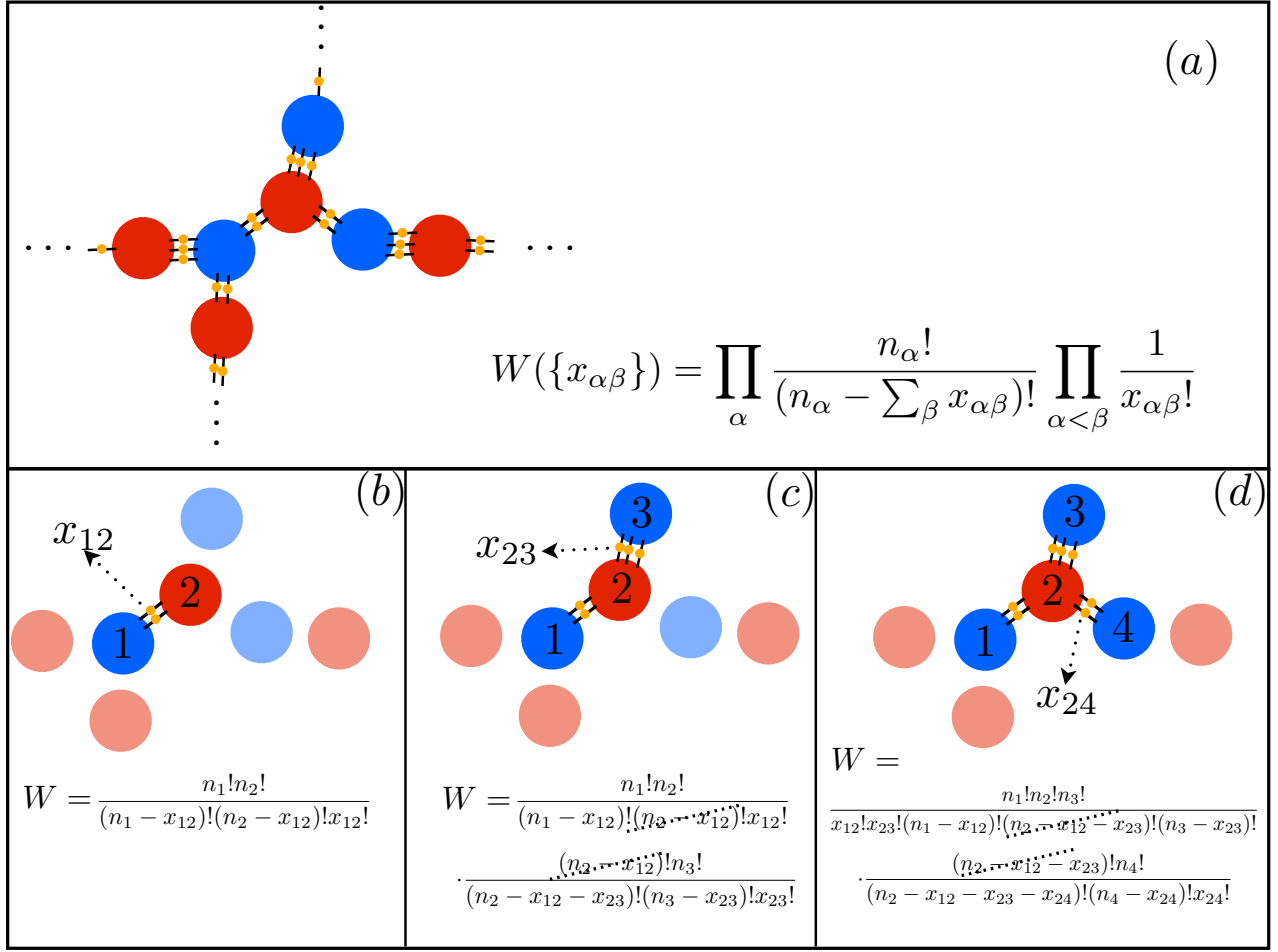


FIG. 6: Counting the number of possible bonds combinations $W(\{x_{\alpha\beta}\})$ in Eq. 20 via combinatorial analysis (see procedure in the main text).

particles. The generalisation to the case in which more than one family of DNA is present on a single colloid is straightforward. Starting from a configuration with no bonds formed (in which $x_{\alpha\beta} = 0$ for all α and β), the number of ways of making x_{12} bridges between particle 1 and particle 2 is given by (see Fig. 6b)

$$W_{12} = \frac{n_1!n_2!}{(n_1 - x_{12})!(n_2 - x_{12})!x_{12}!}.$$

In the previous expression we have accounted for the indistinguishability of the bridges and n_{α} is the total number of linkers present on the particle α . At the next step we count the number of possible combinations resulting in x_{23} bridges between particle 2 and 3 finding

$$W_{23} = \frac{(n_2 - x_{12})!n_3!}{(n_3 - x_{23})!(n_2 - x_{12} - x_{23})!x_{23}!}.$$

resulting in a total number of configurations (see Fig. 6c)

$$W(x_{12}, x_{23}, 0, \dots, 0) = W_1 W_2 = \frac{n_1!}{(n_1 - x_{12})!} \frac{n_2!}{(n_2 - x_{12} - x_{23})!} \frac{n_3!}{(n_3 - x_{23})!} \frac{1}{x_{12}!x_{23}!}.$$

In the previous expression we recognise the factorisation of Eq. 20 in term of type terms (first three terms) and type-type terms (last two term). Recursively adding the missing bridges (e.g. see Fig. 6d for x_{24}) it is easy to see that we obtain an expression for W that remains consistent with Eq. 20.

Using a Stirling approximation we can write the partition function (Eq. 20) as

$$Z = \sum_{\{x_{\alpha\beta}\}} e^{-\beta\mathcal{F}(\{x_{\alpha\beta}\})} \quad (21)$$

$$\beta\mathcal{F}(\{x_{\alpha\beta}\}) = \sum_{\alpha} \left[\sum_{\beta} x_{\alpha\beta} + (n_{\alpha} - \sum_{\beta} x_{\alpha\beta}) \log(n_{\alpha} - \sum_{\beta} x_{\alpha\beta}) - n_{\alpha} \log n_{\alpha} \right]$$

$$+ \sum_{\alpha < \beta} \left[x_{\alpha\beta} \log x_{\alpha\beta} - x_{\alpha\beta} - x_{\alpha\beta} \ln \Xi_{\alpha\beta} \right].$$

In the limit in which $n_{\alpha} \rightarrow \infty$ (with n_{α}/n_{β} fixed) the number of linkers distribution functions peak around the saddle point solution $n_{\alpha\beta}$ defined by

$$\frac{\partial}{\partial x_{\alpha\beta}} \mathcal{F}(n_{\alpha\beta}) = 0. \quad (22)$$

The free energy of the system (βF) is then given by

$$\beta F = \beta\mathcal{F}(\{n_{\alpha\beta}\}) \quad (23)$$

Using Eqs. 22 and 21 we find

$$n_{\alpha\beta} = (n_{\alpha} - \sum_{\gamma} n_{\alpha\gamma})(n_{\beta} - \sum_{\gamma} n_{\beta\gamma}) \Xi_{\alpha\beta}. \quad (24)$$

Now we show that Eq. 24 is equivalent of Eq. 6 in the main text. This can be done identifying the probability that a tethers of type α to be free as

$$p_{\alpha} = \frac{n_{\alpha} - \sum_{\gamma} n_{\alpha\gamma}}{n_{\alpha}} = \frac{\bar{n}_{\alpha}}{n_{\alpha}}$$

where \bar{n}_{α} is the number of tethers of type α unbound. Using p_{α} we can write the tether balance as

$$\bar{n}_{\alpha} + \sum_{\beta} n_{\alpha\beta} = n_{\alpha}$$

$$p_{\alpha} + \sum_{\beta} \frac{n_{\alpha\beta}}{n_{\alpha}} = 1. \quad (25)$$

Using Eq. 24 in Eq. 25 we obtain the same set of equations found in the manuscript

$$p_{\alpha} + \sum_{\beta} n_{\beta} p_{\alpha} p_{\beta} \Xi_{\alpha\beta} = 1 \quad (26)$$

with $\alpha = 1, \dots, N_{\text{type}}$.

We are now in a position to evaluate the free energy 23. Using Eq. 24 we can write

$$\sum_{\alpha < \beta} \left[n_{\alpha\beta} \log n_{\alpha\beta} - n_{\alpha\beta} \log \Xi_{\alpha\beta} \right] = \sum_{\alpha < \beta} n_{\alpha\beta} \left[\log(\bar{n}_{\alpha} \bar{n}_{\beta} \Xi_{\alpha\beta}) - \log \Xi_{\alpha\beta} \right] \quad (27)$$

$$= \sum_{\alpha < \beta} n_{\alpha\beta} \left[\log \bar{n}_{\alpha} + \log \bar{n}_{\beta} \right] \quad (28)$$

$$= \sum_{\alpha, \beta} n_{\alpha\beta} \log \bar{n}_{\alpha} \quad (29)$$

Using the previous equation in 21 we find

$$\beta F = \frac{1}{2} \sum_{\alpha, \beta} n_{\alpha\beta} + \sum_{\alpha} n_{\alpha} \log \frac{\bar{n}_{\alpha}}{n_{\alpha}}$$

$$\beta F = \frac{1}{2} \sum_{\alpha} \left(n_{\alpha} - \bar{n}_{\alpha} + n_{\alpha} \log p_{\alpha} \right)$$

$$\beta F = \frac{1}{2} \sum_{\alpha} n_{\alpha} (1 - p_{\alpha}) + \sum_{\alpha} n_{\alpha} \log p_{\alpha}$$

$$\beta F = \sum_{\alpha} n_{\alpha} [\log(p_{\alpha}) + 1/2 (1 - p_{\alpha})] \quad (30)$$

which again is equivalent to Eq. 7 in the main text.

In Ref.¹⁷, Equations 1-3 of the main text, from which the final self-consistent equations and the free-energy of the system of mobile linkers are obtained here, were derived assuming that the conditional probability for a linker to be unbound given that another one was unbound was independent from the latter. Since for the case of mobile linkers we obtain the same functional equations considering an *exact* partition function, this means that in this latter case the approximation becomes *exact* in the limit where a large number of linkers is present.

C. An analytical expression for F_{clus}

Eq. 8 in the main text can be solved to give:

$$\begin{cases} p_\alpha &= \frac{-1 + \Xi(n_\alpha - N_B n_\beta) + \sqrt{4\Xi n_\alpha + (1 - \Xi(n_\alpha - N_B n_\beta))^2}}{2\Xi n_\alpha} \\ p_\beta &= \frac{-1 + \Xi(N_B n_\beta - n_\alpha) + \sqrt{4\Xi n_\alpha + (1 - \Xi(n_\alpha - N_B n_\beta))^2}}{2\Xi N_B n_\beta} \end{cases} \quad (31)$$

Combining this solution to Eq. 9 in the main text, the following formula arises for the bonding part of the free-energy of a cluster of an A colloid coated with n_α linkers surrounded by N_B neighbours, each coated with n_β linkers, in equivalent positions (linkers α and β are complementary and can form a bond with average energy Ξ , see main text for details).

$$F_{clus} = n_\alpha(A_1 + A_2) + N_B n_\beta(B_1 + B_2) + N_B F_{rep}^{min} \quad (32)$$

$$A_1 = 1/2 \left(1 - \frac{\Xi^{-1}(-1 + \Xi n_\alpha - \Xi N_B n_\beta + \sqrt{4\Xi n_\alpha + (1 + \Xi(-n_\alpha + N_B n_\beta))^2})}{2n_\alpha} \right) \quad (33)$$

$$A_2 = \log \left(\frac{\Xi^{-1}(-1 + \Xi n_\alpha - \Xi N_B n_\beta + \sqrt{4\Xi n_\alpha + (1 + \Xi(-n_\alpha + N_B n_\beta))^2})}{2n_\alpha} \right) \quad (34)$$

$$B_1 = 1/2 \left(1 - \frac{\Xi^{-1}(-1 - \Xi n_\alpha + \Xi N_B n_\beta + \sqrt{4\Xi n_\alpha + (1 + \Xi(-n_\alpha + N_B n_\beta))^2})}{2N_B n_\beta} \right) \quad (35)$$

$$B_2 = \log \left(\frac{\Xi^{-1}(-1 - \Xi n_\alpha + \Xi N_B n_\beta + \sqrt{4\Xi n_\alpha + (1 + \Xi(-n_\alpha + N_B n_\beta))^2})}{2N_B n_\beta} \right) \quad (36)$$